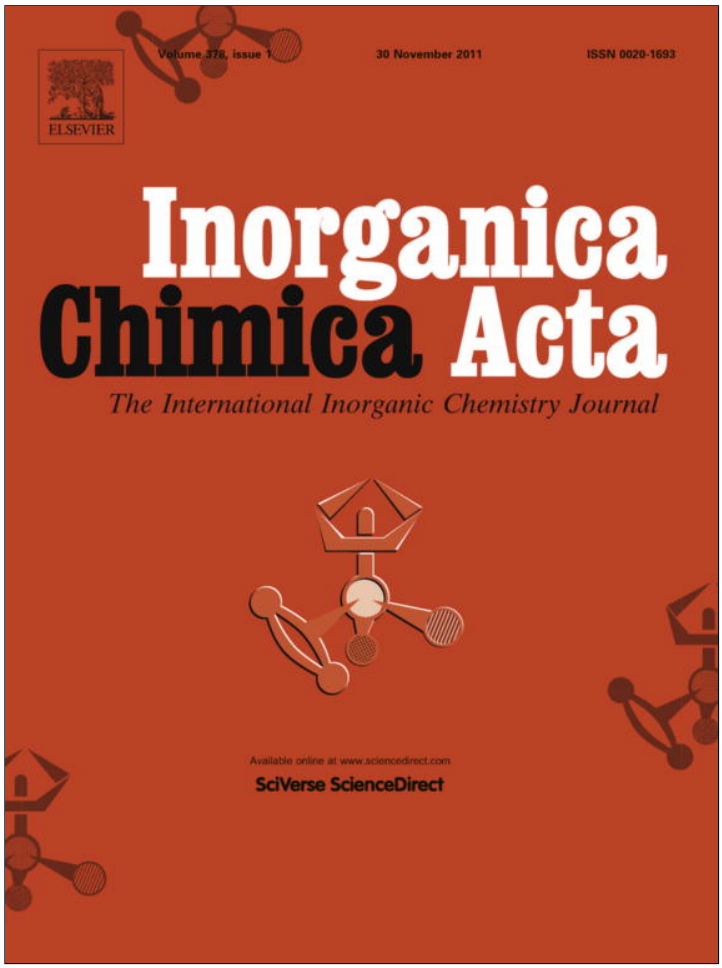

Inorganica Chimica Acta 378 (2011) 115–120

Contents lists available at SciVerse ScienceDirect

Inorganica Chimica Acta

journal homepage: www.elsevier.com/locate/ica

Spectroscopy, electrochemistry, and nucleophilicity of nickel and cobalt complexes of 2′-pyridine carboxaldehyde 2′-pyridyl hydrazone (papyH)

Hoang Nguyen Ly, David J.R. Brook *, Oliver Oliverio

Department of Chemistry, San José State University, One Washington Square, San José, CA 95192-0101, United States

ARTICLE INFO

Article history:
Received 24 September 2010
Accepted 14 August 2011
Available online 9 September 2011

Keywords:
Nickel
Cobalt
Hydrazone
Nucelophilic substitution
p*Ka*

ABSTRACT

Nickel and cobalt complexes of pyridine-2-carboxaldehyde-2′-pyridylhydrazone (papyH) and N-methyl(pyridine-2-carboxaldehyde-2′-pyridyl-hydrazone) (papyMe) have been fully characterized through electrochemistry, titration, and alkylation with methyl iodide and compared with existing data on zinc and iron complexes. Both rate constants for alkylation and ligand p*Ka* depend on the coordinated metal and can be understood based on the influence of *d* electrons on the ligand molecular orbitals.

1. Introduction

Chelating ligands based on hydrazones, such as pyridine-2-carboxaldehyde-2′-pyridylhydrazone (papyH), were first reported over 40 years ago [1–4] and have received sporadic attention since, largely in the context of analytical chemistry [5]. Hydrazone ligands with free NH groups frequently undergo large increases in acidity upon metal coordination [6], and the distinctive UV–Vis spectra of the resulting anion complexes have been advocated as analytical indicators [5]. More recently, hydrazones have gained attention as analogs of polypyridyl ligands that can undergo self-assembly to form polymetallic grid structures [7–11]. In this context, the facile synthesis of the hydrazone link compared with the corresponding polypyridines greatly facilitates the formation of a broad variety of ligands. Similarly, the reversible nature of hydrazone formation has allowed the synthesis of dynamic molecular libraries that can be driven toward particular systems using pressure for metal coordination [12,13]. Deprotonation of the hydrazone ligand can drive self-assembly [11] and has also been utilized to selectively synthesize polymetallic grid complexes via manipulation of redox states and corresponding barriers to ligand exchange [10]. Furthermore, the nucleophilic nature of the coordinated hydrazone anion provides a further potential avenue for the elaboration of self-assembled units [14].

In a parallel, but far less explored avenue of research, one of the original reports of hydrazone ligands also mentioned that transition metal complexes of di(2-pyridylmethyl)amine could be deprotonated to produce highly colored compounds, but the products were too unstable to characterize [2,3]. Far more recently, Wolczanski and co-workers rediscovered this observation and characterized a series of transition metal complexes of the 1,3-dipyridyl-2-azaallyl or 'smif' ligand, which is isoelectronic with the corresponding hydrazone [15,16].

Despite this recent and expanding interest, the electronic properties of simple hydrazone complexes are still relatively poorly understood. Though complexes have been reported for a number of transition metals, early characterization has been incomplete (for example, redox properties were not reported) and in some cases, misleading (the $Fe(papy)_2$ complex was originally reported as paramagnetic). We have started to fill this void with a detailed investigation of the properties and reactivity of the iron complex of papy [14]. We now expand our investigation with a study on the corresponding cobalt and nickel complexes including a detailed analysis of their spectroscopy, electrochemistry, and nucleophilicity.

2. Experimental

2.1. General

Pyridine-2-carboxaldehyde-2′-pyridylhydrazone (papyH) was synthesized as reported by Geldard and Lions [2] and recrystallized from ethanol. Tetrakis(acetonitrile) cobalt(II) triflate and tetrakis(acetonitrile) nickel(II) triflate were synthesized from the metals and triflic acid in acetonitrile according to literature procedures.

* Corresponding author. Tel.: +1 408 924 4994; fax: +1 408 924 4945.
E-mail address: dbrook@science.sjsu.edu (D.J.R. Brook).

0020-1693/$ - see front matter © 2011 Elsevier B.V. All rights reserved.
doi:10.1016/j.ica.2011.08.037

2.2. N-methyl(pyridine-2-carboxaldehyde-2′-pyridyl-hydrazone), (papyMe)

Pyridine-2-carboxaldehyde-2′-pyridyl-hydrazone (0.0411 g, 0.207 mmol), papy-H, was dissolved in 60 mL of tetrahydrofuran with stirring. Excess sodium hydride was added to the solution followed by an excess iodomethane. The solution was stirred for an hour and was poured into 150 mL of deionized water. The solution was extracted with three 150 mL portions of dichloromethane. The organic extract was dried over sodium sulfate, and the solvent was removed by evaporation. The product was further purified with washes of hexanes and dried under vacuum for 6 hours (0.0449 g, 0.212 mmol, 92% yield). EI-MS *m*/*z* (rel intensity) 212 (M^+, 11), 134 (100), 107 (7), 78 (17), 51 (6). M.p. 100.0–102.2 °C. IR (NaCl plate) 1590, 1480, 1460, 1430, 1380, 1130, 980, 774. ^{1}H NMR (300 MHz, $CDCl_3$): 8.1 (m, 2H), 7.7 (m 2H), 7.5 (m, 2H), 7.1 (m, 2H), 6.7 (m, 2H), 6.3 (m, 2H), 3.2 (s, 8H), 1.2 (s, 2H), 0.7 (s, 1H). ^{13}C NMR (75 MHz, $CDCl_3$): 155.6, 149.4, 147.2, 137.8, 136.5, 134.9, 122.7, 119.5, 116.4, 110.3, 29.9. UV–Vis (acetonitrile) λ_{max} (ε_{max}) 227 nm (14000 L mol^{-1} cm^{-1}), 333 (17200).

2.3. Ni(papyMe)$_2$(PF_6^-)$_2$

papyMe (0.0047 g, 0.022 mmol) was dissolved in acetonitrile. Nickel triflate (0.0038 g, 0.011 mmol) was dissolved in acetonitrile and was added to the papyMe solution. The solvent was removed by evaporation, and the residue was dissolved in methanol. An excess of ammonium hexafluorophosphate was dissolved in methanol and was added to the solution. The crude Ni(papyMe)$_2$(PF_6^-)$_2$ was removed by filtration. The product was purified by diffusion of ether into an acetonitrile solution (0.0014 g, 0.0078 mmol, 40% yield). ES-MS *m*/*z*: 482.9. IR (NaCl plate) 1590, 1440, 1320, 1150, 1010, 829, 769. ^{1}H NMR (300 MHz, CD_3CN): 83.3 (s, 1H), 64.6 (s, 1H), 51.4 (s, 1H), 39.1 (s, 1H), 18.5 (s, 1H), 12.9 (s, 1H), 11.2 (s, 1H), 1.9 (s, 9H). ^{1}H NMR (300 MHz, CD_3CN, 25 °C): 82.1 (s, 1H), 64.3 (s, 1H), 51.1 (s, 1H), 39.0 (s, 1H), 18.6 (s, 3H), 13.1 (s, 1H), 11.4 (s, 1H), 1.9 (s, 9H). ^{1}H NMR (300 MHz, CD_3CN, 50 °C): 75.8 (s, 1H), 59.6 (s, 1H), 47.4 (s, 1H), 36.3 (s, 1H), 17.4 (s, 3H), 12.6 (s, 1H), 11.0 (s, 1H), 1.9 (s, 9H). ^{1}H NMR (300 MHz, CD_3CN, 75 °C): 70.6 (s, 1H), 55.8 (s, 1H), 44.6 (s, 1H), 34.3 (s, 1H), 16.5 (s, 3H), 12.4 (s, 1H), 10.9 (s, 1H), 2.1 (s, 9H). UV–Vis (CH_3CN) λ_{max} (ε_{max}) 259 nm (24400 L mol^{-1} cm^{-1}), 368 (39900); $\chi_{mol}T$ = 1.34 (294 K).

2.4. Ni(papy)$_2$

This compound was synthesized as described by Geldard and Lions and recrystallized from toluene. Previously unrecorded spectral data are recorded below. ES-MS *m*/*z*: 453.0. IR (NaCl plate) 1593, 1452, 1415, 1292, 1247, 1129, 997. ^{1}H NMR (300 MHz, CD_3CN, 25 °C): 60.5 (s, 1H), 57.5 (s, 1H), 54.1 (s, 1H), 48.9 (s, 1H), 10.9 (s, 1H), 9.3 (s, 1H), 7.0 (s, 1H), 1.9 (s, 9H). ^{1}H NMR (300 MHz, CD_3CN, 40 °C): 57.7 (s, 1H), 54.7 (s, 1H), 51.6 (s, 1H), 46.8 (s, 1H), 10.6 (s, 1H), 9.2 (s, 1H), 7.0 (s, 1H), 1.9 (s, 9H). ^{1}H NMR (300 MHz, CD_3CN, 55 °C): 55.2 (s, 1H), 52.3 (s, 1H), 49.4 (s, 1H), 44.8 (s, 1H), 10.3 (s, 1H), 9.1 (s, 1H), 7.0 (s, 1H), 1.9 (s, 9H). UV–Vis (acetonitrile) λ_{max} (ε_{max}) 326 nm (28100 L mol^{-1} cm^{-1}) 477 (29900); $\chi_{mol}T$ = 1.05 (295 K).

2.5. Co(papyMe)$_2$(PF_6^-)$_2$

papyMe (0.0045 g, 0.021 mmol) was dissolved in acetonitrile. Cobalt triflate (0.0036 g, 0.010 mmol) was dissolved in acetonitrile and was added to the papyMe solution. The solvent was removed by evaporation and the residue was dissolved in methanol. An excess of ammonium hexafluorophosphate was dissolved in methanol and was added to the solution. The crude Co(papyMe)$_2$(PF_6^-)$_2$ was removed by filtration. The product was purified by diffusion of ether into an acetonitrile solution (0.0031 g, 0.017 mmol, 94% yield). ES-MS *m*/*z*: 241.6. IR (NaCl plate) 1580, 1430, 1320, 1150, 818, 766. ^{1}H NMR (300 MHz, CD_3CN, 25 °C): 188.6 (s, 1H), 151.1 (s, 1H), 141.8 (s, 1H), 78.6 (s, 1H), 60.6 (s, 1H), 52.7 (s, 1H), 46.1 (s, 1H), 10.9 (s, 1H), 2.0 (m, 9H). ^{1}H NMR (300 MHz, CD_3CN, 50 °C): 177.0 (s, 1H), 139.3 (s, 1H), 132.7 (s, 1H), 73.7 (s, 1H), 56.5 (s, 1H), 49.4 (s, 1H), 43.1 (s, 1H), 10.7 (s, 1H), 1.9 (s, 9H). ^{1}H NMR (300 MHz, CD_3CN, 75 °C): 166.6 (s, 1H), 129.3 (s, 1H), 124.4 (s, 1H), 69.5 (s, 1H), 52.9 (s, 1H), 46.4 (s, 1H), 40.5 (s, 1H), 10.1 (s, 1H), 1.9 (m, 9H). UV–Vis (CH_3CN) λ_{max} (ε_{max}) 292 nm (15200 L mol^{-1} cm^{-1}), 357 (23300); $\chi_{mol}T$ = 2.17 (297 K).

2.6. Oxidation of [Co(papyMe)$_2$]$^{2+}$ with Cu^{2+} in acetonitrile

Co(papyMe)$_2$(PF_6^-)$_2$ (0.0435 g, 0.0562 mmol) was dissolved in acetonitrile. Copper(II) triflate (0.0439 g, 0.123 mmol) was dissolved in acetonitrile and was added to the Co(papyMe)$_2$ (PF_6^-)$_2$ solution. The solvent was evaporated off, and the residue redissolved in CD_3CN for NMR and UV–Vis: ^{1}H NMR (300 MHz, CD_3CN): 9.1 (s, 1H), 8.2 (d, 1H), 8.0 (s, 1H), 7.8 (d, 1H), 7.5 (t, 1H), 7.3 (d, 1H), 7.1 (t, 1H), 6.2 (s, 1H), 6.1 (s, 1H), 5.9 (s, 1H), 4.3 (s, 3H), 2.1 (s, 3H), 1.9 (s, 9H). UV–Vis (CH_3CN) λ_{max} (ε_{max}) 388 nm (19500 L mol^{-1} cm^{-1}).

2.7. Co(papy)$_2^+$$PF_6^-$

papyH (1.0 g, 5 mmol) was dissolved in 20 mL methanol. To this solution was added cobalt(II) nitrate hexahydrate (0.73 g, 2.5 mmol) in 1 mL methanol to form a dark red solution. The solution was made basic with 1 M aqueous NaOH and then evaporated until a crystalline solid began to separate. This was removed by filtration and washed with 10 mL H_2O. The crude Co(papy)$_2^+$$NO_3^-$ was converted to the hexafluorophosphate salt by dissolution in methanol and precipitation with excess ammonium hexafluorophosphate. EC-MS *m*/*z*: 453.0. IR (NaCl plate) 1420, 1300, 1130, 835. ^{1}H NMR (300 MHz, Acetone-D): 7.3 (s, 3H), 6.7 (q, 6H), 6.5 (d, 3H), 6.3 (t, 3H), 6.2 (d, 3H), 6.0 (t, 3H), 5.7 (d, 3H), 5.4 (t, 3H), 4.4 (s, 3H), 1.6 (s, 6H) 0.8 (m, 18H). UV–Vis (acetonitrile) λ_{max} (ε_{max}) 309 nm (22500 L mol^{-1} cm^{-1}), 489 (26600); $\chi_{mol}T$ = −0.072 (295 K).

2.8. Kinetic experiments

Samples of the metal papy complex were dissolved in acetonitrile and an excess of methyl iodide added. UV–Vis spectra were recorded at appropriate intervals until no further change in the spectrum was apparent. Data were analyzed using the method described by Wood et al. [14] to give rate constants for the consecutive alkylation reactions.

The experiment with Co(papy)$_2^+$ was repeated in CD_3CN monitoring by ^{1}H NMR. As the reaction proceeded, it became clear that the final product was the paramagnetic Co(II) complex, indicated by paramagnetic NMR resonances matching those of the sample synthesized by independent means.

3. Results

The ligand, papyH, along with its cobalt and nickel complexes was synthesized using literature procedures. Co(papy)$_2$ and [Co(papyH)$_2$]$^{2+}$ were not isolated because of their air sensitivity; rather atmospheric oxidation in water gave the Co(III) cation [Co(papy)$_2$]$^+$, which was precipitated as the PF_6^- salt. The

methylated ligand, papyMe, was synthesized from papyH by deprotonation with sodium hydride and alkylation with methyl iodide. The cobalt and nickel complexes of papyMe were obtained from the respective metal triflates (Scheme 1)

All complexes were characterized by magnetic susceptibility, ^{1}H NMR, UV–Vis, cyclic voltammetry, and mass spectrometry. Results are summarized in Tables 1–4. Reaction of Ni(papy)$_2$ and [Co(papy)$_2$]$^+$ with excess CH_3I was followed by UV–Vis spectrophotometry. In the case of the nickel complex, data was fitted to a consecutive first-order model to obtain rate constants for the reaction. The fitting procedure (described in Wood et al. [14]) also gave the UV–Vis spectra for the intermediate [Ni(papy)(papyMe)]$^{n+}$ complex and the final product [Ni(papyMe)$_2$]$^{2+}$. The latter spectrum was consistent with the spectrum of [Ni(papyMe)$_2$]$^{2+}$ synthesized by direct combination of metal and ligand. UV–Vis spectra of the various Ni species are shown in Fig. 1.

For alkylation of [Co(papy)$_2$]$^+$, a similar approach was taken and a good fit to a consecutive pseudo first-order model was obtained. However, the UV–Vis spectrum of the product was more consistent with formation of the Co(II) compound [Co(papyMe)$_2$]$^{2+}$ rather than the expected [Co(papyMe)$_2$]$^{3+}$, presumably as a result of oxidation of I^-. Further investigation by NMR confirms that the final product is [Co(papyMe)$_2$]$^{2+}$ by comparison with authentic samples. Furthermore, the presence of sharp NMR signals arising from a diamagnetic intermediate indicates that the reduction to Co(II) occurs after the second alkylation (Fig 2). Rate constants are summarized in Table 1 along with their counterparts for the reaction with Fe(papy)$_2$.

Spectrophotometric titration of [Co(papy)$_2$]$^+$ in methanol/water was used to estimate the two acidity constants for this complex. While we are reasonably confident in the second constant, determination of the first constant was complicated by the known problems of glass electrodes at very low pH (~0). Nevertheless, the values that best fit our data (shown in Table 2) are consistent with other papyH complexes (in that they are separated by ~1–2 pKa units) and the extrapolated UV–Vis spectrum of [Co(papyH)$_2$]$^{3+}$ is almost identical to the measured spectrum of [Co(papyMe)$_2$]$^{3+}$ (Fig 3). Consequently, we believe these values are reasonable approximations. UV–Vis spectra of Co(III) papy species determined by titration are shown in Fig. 3.

Use of these values, in conjunction with the redox potentials, allow estimation of the sum of the acidity constants of [Co(papyH)$_2$]$^{2+}$. Similarly, we have calculated the sum of the acidity constants of [Fe(papyH)$_2$]$^{3+}$. Previous measurements of the Zn, Fe(II), and Ni(II) systems suggest that the consecutive acidity constants differ by approximately one pKa unit. Assuming this holds for the Fe(III) and Co(II) complexes, we have estimated pKa1 and pKa2 for these systems. These values, along with measured values from the literature and our work, are presented in Table 3.

Table 1
Rate constants for alkylation of [M(papy)$_2$]$^{n+}$ systems with methyl iodide.

	$k_1 \times 103$ mol^{-1} s^{-1}	$k_2 \times 103$ mol^{-1} s^{-1}
Ni(papy)$_2$	8.2	0.95
[Co(papy)$_2$]$^+$	0.1	0.02
Fe(papy)$_2$	2.7	0.19

Table 2
Oxidation and reduction potentials for [M(papy)$_2$]$^{n+}$ species and select reference compounds reported vs. ferrocene/ferricenium (Fc/Fc$^+$).

Redox couple	$E_{1/2}$	ΔE_{pp} (mV)	References
[Co(papyMe)$_2$]$^{2+}$/[Co(papyMe)$_2$]$^{3+}$	−0.06	90	
[Co(papyMe)$_2$]$^+$/[Co(papyMe)$_2$]$^{2+}$	−1.15	80	
Co(papy)$_2$/[Co(papy)$_2$]$^+$	−0.43	320	
[Fe(papyH)$_2$]$^{2+}$/[Fe(papyH)$_2$]$^{3+}$	+0.66		[14]
Fe(papy)$_2$/[Fe(papy)$_2$]$^+$	−0.25		[14]
[Fe(terpy)$_2$]$^{2+}$/[Fe(terpy)$_2$]$^{3+}$	+0.98		[18]
[Co(terpy)$_2$]$^{2+}$/[Co(terpy)$_2$]$^{3+}$	−0.05		[18]
[Fe(phen)$_3$]$^{2+}$/[Fe(phen)$_3$]$^{3+}$	+0.87		[20]
[Co(terpy)$_2$]$^+$/[Co(terpy)$_2$]$^{2+}$	−1.2		[18]

(Fc/Fc$^+$ = +0.64 vs. NHE, +0.4 vs. SCE).

Table 3
Measured or calculated values of p*K*a for [M(papyH)$_2$]$^{n+}$ species.

Species	pK_{a1}	pK_{a2}	pK_{a1} + pK_{a2}	References
[Fe(papyH)$_2$]$^{2+}$	5.68	6.57	12.25	[4]
[Co(papyH)$_2$]$^{2+}$	~6.3[b]	~7.3[b]	13.6[a]	this work
[Ni(papyH)$_2$]$^{2+}$	7.37	8.5	15.87	[4,21]
[Zn(papyH)$_2$]$^{2+}$	7.94	8.85	16.79	[4]
[Fe(papyH)$_2$]$^{3+}$	~1.5[b]	~2.5[b]	4[a]	this work
[Co(papyH)$_2$]$^{3+}$	~0	1.7	1.7	this work

[a] Value calculated from redox potentials.
[b] Value calculated assuming a difference of 1 between successive pK_a values.

Table 4
Measured and previously reported effective magnetic moment (reported as χT at 298 K) for Co and Ni papy complexes.

Species	χT (295 K)	Literature value	Reference
[Ni(papyMe)$_2$](PF$_6^-$)$_2$	1.34	1.2	[19]
[Co(papyMe)$_2$](PF$_6^-$)$_2$	2.18	–	
Ni(papy)$_2$	1.05	1.05	[3]
[Co(papy)$_2$]$^+$PF$_6^-$	−0.072	0	[1]

4. Discussion

Though the majority of the papy complexes here have been reported previously, the more complete set of thermodynamic and kinetic data presented here provide a comprehensive overview of the role of metal *d* orbital configuration on ligand reactivity. The ligand itself, papyH, is isoelectronic with the recently reported ligand 'smif' and thus would be expected to have a similar orbital structure. A simple 'back of the envelope' analysis suggests that the diaza-allyl unit (or aza-allyl unit in the case of 'smif') should have a non-bonding HOMO with a node at the central coordinating nitrogen. In the case of papyH, the non-bonding orbital is the nitrogen lone pair, which is delocalized onto the imine carbon.

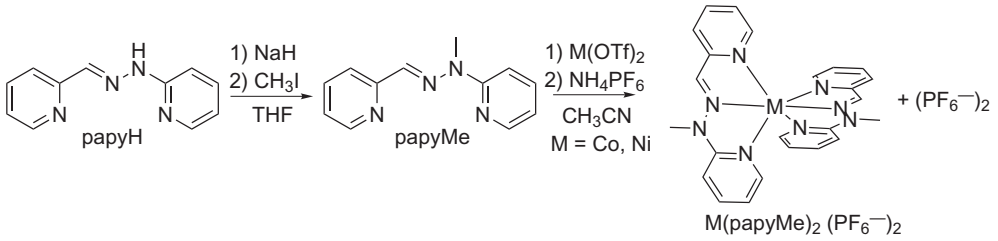

Scheme 1. Synthesis of papyMe and metal complexes of papyMe.

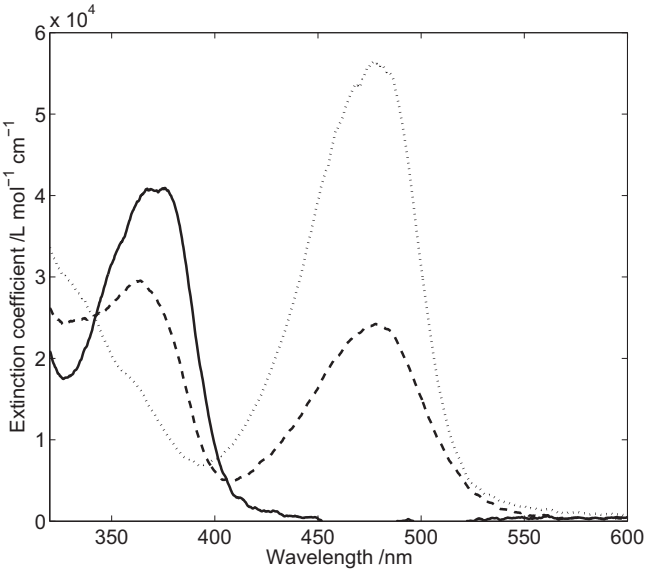

Fig. 1. Visible spectra of $Ni(papy)_2$ (dotted line), $[Ni(papy)(papyMe)]^+$ (dashed line), and $[Ni(papyMe)_2]^{2+}$ (solid line) determined by analysis of kinetic data.

Semi-empirical (AM1) and *ab-initio* [14] calculations support this analysis, with the additional observation that in papy the LUMO and next highest HOMO (HOMO−1) are delocalized onto the aldehyde derived, and hydrazine derived pyridine rings respectively (Fig 4).

Computational studies have also provided a model for the enhancement of ligand acidity observed upon metal coordination and suggest it is a result of interactions through the ligand σ framework. Coordination of a metal ion to the imine nitrogen withdraws electron density from the NH bond via intervening σ bonds and increases its acidity. Upon deprotonation, the new lone pair is in the plane of the ligand where it inductively increases the basicity of the imine nitrogen [14]. This effect drives the self-assembly of zinc-hydrazone grids in DMSO [11]. The interaction of this high-energy σ orbital with metal *d* orbitals influences much of the changes in chemical properties of the complexes passing along the first row transition series.

4.1. Electronic spectra

In the electronic spectra of Ni(papy/papyH/papyMe) and Co(papy/papyH/papyMe) systems, a single intense band was observed that underwent a red shift of ~100 nm upon moving from neutral to anionic ligands. Intermediate $[M(papy)(papyR)_2]^{n+}$ species show both bands suggesting that the bands are intraligand π–π^* transitions. The spectra are very similar to those observed for $Co(smif)_2$ and $Ni(smif)_2$ [16], and in fact, computational results indicate the 'smif' ligand and papy both have very similar energy frontier orbitals. They also make a distinct contrast with the spectra of the corresponding iron complexes that are dominated by metal-ligand charge transfer bands. $Fe(smif)_2$ shows a complex UV–Vis spectrum [16], and while the spectrum of $Fe(papyR)_x$ is simpler, the shift in position of the band rather than its growth or decay upon alkylation indicates that this band is most likely due to metal ligand charge transfer [14].

4.2. Magnetochemistry

Not surprisingly, all the reported Co(III) complexes are diamagnetic, consistent with earlier results. The Co(II) complex, $[Co(papyMe)_2]^{2+}(PF_6)_2$, is high spin at room temperature (Table 4) unlike $Co(papy)_2$, which shows an equilibrium between low and high temperature forms [17]. Though a spin crossover at lower temperatures has not been ruled out, ^{1}H NMR chemical shifts increase with decreasing temperature to 0 °C with no indication of spin crossover. This is consistent with the orbital model; the weaker σ donation of the methylated ligand favoring the high spin form. Our measurements confirm previously reported values for the nickel complexes but we note that they are also consistent with the orbital model; χT for $Ni(papy)_2$ is closer to the spin only value

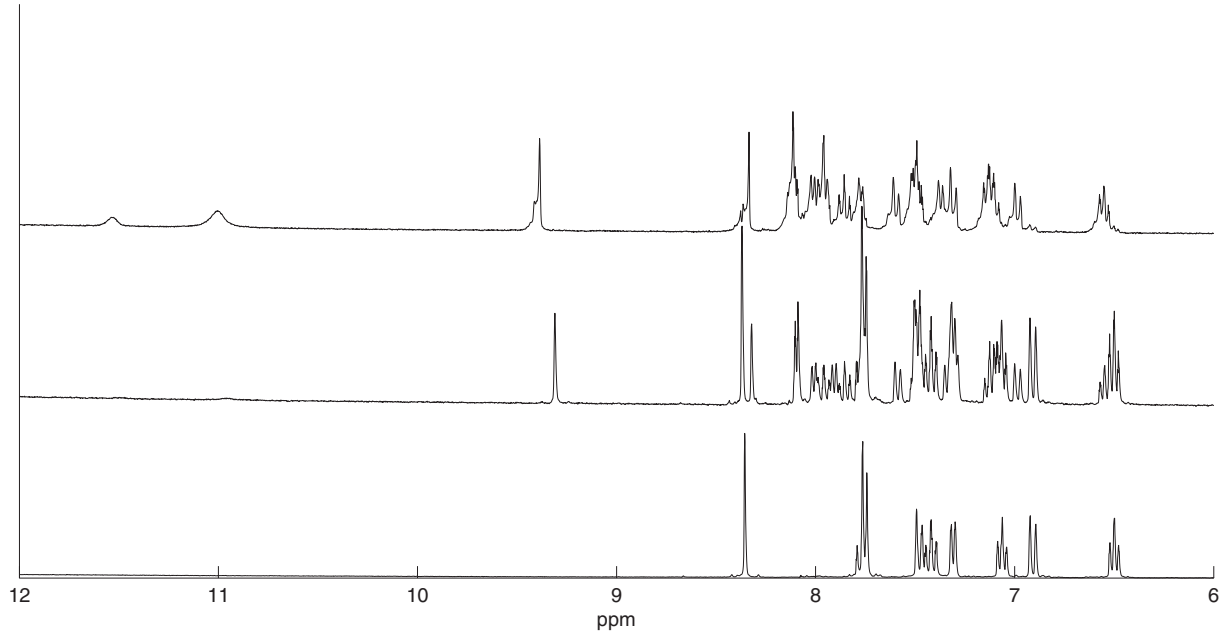

Fig. 2. ^{1}H NMR spectra recorded during the alkylation of $[Co(papy)_2]^+$ with methyl iodide. Bottom: spectrum of $[Co(papy)_2]^+$ at the start of the reaction. Middle: after 38 h, additional resonances due to $[Co(papy)(papyMe)]^{2+}$ are apparent. Top: after 180 h $[Co(papy)_2]^+$ has been consumed. Resonances from $[Co(papy)(papyMe)]^{2+}$ are still visible along with broad peaks from the paramagnetic $[Co(papyMe)_2]^{2+}$.

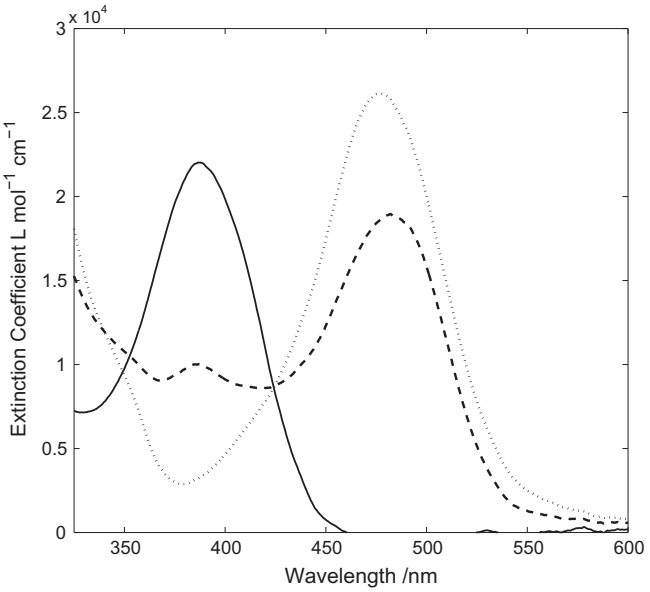

Fig. 3. Visible spectra of $[Co(papy)_2]^+$ (dotted line), $[Co(papyH)(papy)]^{2+}$ (dashed line), and $[Co(papyH)_2]^{3+}$ (solid line) determined by titration.

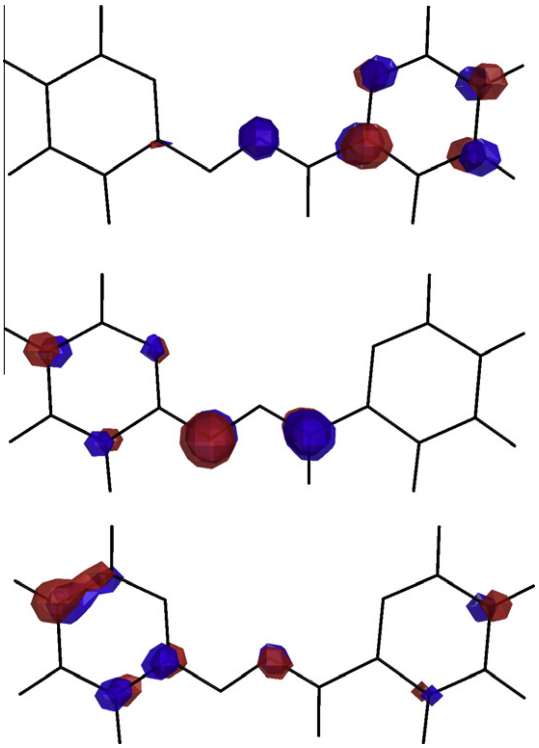

Fig. 4. Frontier orbitals for papy anion. From top to bottom: LUMO, HOMO, HOMO−1.

as a result of more effective quenching of orbital angular momentum caused by the stronger ligand field.

4.3. Electrochemistry

Though the Ni compounds show no clean reversible electrochemistry, reversible one electron processes are observed for the cobalt complexes. Oxidation and reduction of $[Co(papyMe)_2]^{2+}$ are observed at potentials very similar to the corresponding cobalt bis-terpyridine complex [18]. As in the Fe system [14], anionic ligands reduces the oxidation potential, but to a lesser extent (0.4 V versus 0.9 V). The difference reflects a weaker metal ligand interaction that has also been noted in the discussion of electronic spectroscopy (*vide supra*). The corresponding (protonated) cobalt(II) hydrazone grid complex shows a much higher oxidation potential reflecting the effect of the high positive charge on the grid [8,9], though surprisingly no reversible oxidation was observed for the cobalt methylated hydrazone grid. We are not certain of the cause of this discrepancy.

4.4. Acidity

Passing from Fe(II) to Zn(II) results in a steady reduction in the acidity of the metal complexes (Table 3, above). This corresponds to increasing occupation of the metal d_σ orbitals, raising the energy of the L_σ orbital and thus reducing the stability of the deprotonated form of the ligand. To our knowledge, no p*K*a values of trivalent papyH coordination compounds have been previously reported. As might be expected with an increase in Lewis acidity and charge of the metal ion, the M^{3+} complexes are significantly more acidic; with a first p*K*a near zero the Co(III) complex is a strong acid. With the trivalent ions, however, the order of acidity is reversed, and the Co(III) compound is more acidic than the Fe(III) compound. In neither of these compounds are the d_σ orbitals occupied. The increase in acidity in the Co(III) system results from a decrease in energy of the empty d_σ orbitals, and thus reducing the energy of the overlapping ligand σ orbital.

4.5. Alkylation

Alkylation of papy complexes has been previously reported for iron [14] and nickel [19] complexes, but not the Co(III) system. Earlier studies with nickel and alkyl chlorides resulted in displacement of the papyMe ligand by chloride ion. Rates of alkylation have only previously been determined for the Fe system. Rates of alkylation of the coordinated papy anion follow the corresponding pKa. The Ni compound shows the highest pKa and is alkylated faster than the Fe compound. While data for the Co(II) compound is unavailable, the Co(III) compound is alkylated far more slowly, consistent with the far lower basicity for this compound. The straightforward nucleophilic behavior of the coordinated (and uncoordinated) papy anion contrasts with the rather unusual dimerization observed for the mono-smif complex of Fe.

5. Conclusion

Though transition metal complexes of papy have been known for over 40 years, a detailed understanding of the interaction of metal and ligand orbitals has been lacking. Our studies complete the known data on cobalt and nickel complexes and complement the existing data on the iron complexes with illustrations of how occupation of the metal *d* orbitals influences both metal and ligand properties. This understanding will be important in the utilization of hydrazone ligands in molecular devices.

References

[1] B. Chiswell, F. Lions, J.F. Geldard, A.T. Phillip, Inorg. Chem. 3 (1964) 1272.
[2] J.F. Geldard, F. Lions, J. Am. Chem. Soc. 84 (1962) 2262.
[3] J.F. Geldard, F. Lions, Inorg. Chem. 2 (1963) 270.
[4] R.W. Green, P.S. Hallman, F. Lions, Inorg. Chem. 3 (1964) 376.
[5] T. Taya, Bunseki Kagaku. 45 (1996) 109.
[6] R.W. Green, W.G. Goodwin, Aust. J. Chem. 21 (1968) 1165.
[7] M. Ruben, J. Rojo, F.J. Romero-Salguero, L.H. Uppadine, Jean-Marie Lehn, Angew. Chem., Int. Ed. 43 (2004) 3644.
[8] L.H. Uppadine, J.P. Gisselbrecht, N. Kyritsakas, K. Nattinen, K. Rissanen, J.M. Lehn, Chem. Eur. J. 11 (2005) 2549.

[9] L.H. Uppadine, J.P. Gisselbrecht, J.M. Lehn, Chem. Commun. (2004) 718.
[10] L.H. Uppadine, J.M. Lehn, Angew. Chem., Int. Ed. 43 (2004) 240.
[11] M. Barboiu, M. Ruben, G. Blasen, N. Kyritsakas, E. Chacko, M. Dutta, O. Radekovich, K. Lenton, D.J.R. Brook, J.M. Lehn, Eur. J. Inorg. Chem. (2006) 784.
[12] Cheuk-Fai Chow, Shunsuke Fujii, Jean-Marie Lehn, Angew. Chem., Int. Ed. 46 (2007) 5007.
[13] C.F. Chow, S. Fujii, J.M. Lehn, Chem. Asian J. 3 (2008) 1324.
[14] A. Wood, W. Aris, D.J.R. Brook, Inorg. Chem. 43 (2004) 8355.
[15] B.A. Frazier, P.T. Wolczanski, E.B. Lobkovsky, Inorg. Chem. 48 (2009) 11576.
[16] B.A. Frazier, P.T. Wolczanski, E.B. Lobkovsky, T.R. Cundari, J. Am. Chem. Soc. 131 (2009) 3428.
[17] A.M. Vecchio-Sadus, Transition Met. Chem. 20 (1995) 38.
[18] J. Chambers, B. Eaves, D. Parker, R. Claxton, P.S. Ray, S.J. Slattery, Inorg. Chim. Acta 359 (2006) 2400.
[19] D.S. Black, R.C. Srivastava, Aust. J. Chem. 24 (1971) 287.
[20] P.S. Braterman, J.I. Song, R.D. Peacock, Inorg. Chem. 31 (1992) 555.
[21] T. Taya, T. Sakamoto, K. Doi, M. Otomo, Bull. Chem. Soc. Jpn. 66 (1993) 3652.